

Anomalous relaxation and the high-temperature structure factor of XXZ spin chains

Sarang Gopalakrishnan^{a,b,1}, Romain Vasseur^c, and Brayden Ware^{c,d}

^aDepartment of Physics and Astronomy, City University of New York College of Staten Island, Staten Island, NY 10314; ^bPhysics Program and Initiative for the Theoretical Sciences, The Graduate Center, City University of New York, New York, NY 10016; ^cDepartment of Physics, University of Massachusetts, Amherst, MA 01003; and ^dRudolf Peierls Centre for Theoretical Physics, Clarendon Laboratory, University of Oxford, Oxford OX1 3PU, United Kingdom

Edited by Subir Sachdev, Harvard University, Cambridge, MA, and approved July 1, 2019 (received for review April 22, 2019)

We compute the spin-structure factor of XXZ spin chains in the Heisenberg and gapped (Ising) regimes in the high-temperature limit for nonzero magnetization, within the framework of generalized hydrodynamics, including diffusive corrections. The structure factor shows a hierarchy of timescales in the gapped phase, owing to s -spin magnon bound states ("strings") of various sizes. Although short strings move ballistically, long strings move primarily diffusively as a result of their collisions with short strings. The interplay between these effects gives rise to anomalous power-law decay of the spin-structure factor, with continuously varying exponents, at any fixed separation in the late-time limit. We elucidate the cross-over to diffusion (in the gapped phase) and to superdiffusion (at the isotropic point) in the half-filling limit. We verify our results via extensive matrix product operator calculations.

spin transport | integrable systems | anomalous diffusion | matrix product operators

Many experimentally relevant 1D systems are described by approximately integrable models, such as the Hubbard, Heisenberg, and Lieb–Liniger models (1–3). The nonequilibrium dynamics of integrable systems, their failure to thermalize, and their possession of an extensive set of conservation laws have been explored extensively (4–7). [In experiments, integrability is approximate and gives rise to "prethermal" intermediate-time regimes of effectively integrable dynamics (8–10).] Integrable systems support stable, ballistically propagating quasiparticles, even at high temperature. In the simplest cases (e.g., free fermions), these particles carry the same quantum numbers as the microscopic degrees of freedom and move with a velocity set by the band structure. In *interacting* integrable models, however, each quasiparticle is dressed by all of the others (11). This dressing can lead to remarkable dynamical effects, for instance, in the "gapped" phase of the XXZ model considered here: Even though quasiparticles move ballistically, finite-temperature spin transport is diffusive in the absence of an external field (12–25).

Recently, a coarse-grained approach to integrable dynamics has been developed; this approach is termed "generalized hydrodynamics" (GHD) (refs. 26 and 27; see also refs. 19, 20, and 28–44). A core insight of GHD is that an integrable system can be mapped to an appropriate classical soliton gas (32). Assuming the system is initially in local equilibrium, the velocities of these solitons can be computed by using the thermodynamic Bethe ansatz (26, 27, 45), which is much more tractable than exactly simulating the full dynamics. In the initial formulation of GHD, the dressing of quasiparticles by interactions was treated at the "Euler" level, yielding purely ballistic hydrodynamics; recently, adding Gaussian fluctuations on top of this treatment was shown to give diffusive corrections to hydrodynamics (21–24). Diffusive corrections generically occur on top of ballistic transport; however, when the ballistic term is absent, transport is dominated by diffusion.

In this work, we show that even when ballistic transport is present, correlation functions can decay with anomalous exponents. We focus on the XXZ spin chain:

$$H = \sum_i [S_i^x S_{i+1}^x + S_i^y S_{i+1}^y + \Delta S_i^z S_{i+1}^z], \quad [1]$$

where $S_i^\alpha = \frac{\sigma_i^\alpha}{2}$ are spin- $\frac{1}{2}$ operators. We are concerned with the case of easy-axis anisotropy $|\Delta| \geq 1$ at infinite temperature (so the sign of Δ is irrelevant). We define $\eta \equiv \cosh^{-1} \Delta$. The model has a conserved magnetization, $\sigma_{\text{tot}}^z = \sum_i \sigma_i^z$; we denote the associated magnetization density as $h = \tanh \mu$, corresponding to a filling $f = (1+h)/2$. At half-filling ($h=0$), ballistic transport is absent because the propagating quasiparticles carry no spin. One can easily see this for magnons in the ferromagnetic phase at low but nonzero temperatures: A magnon propagates as a \downarrow spin through a domain of \uparrow spins, then continues as an \uparrow spin through a domain of \downarrow spins, etc., so on average it does not carry magnetization. This result, which holds generally, was first noted in the low-temperature limit (13, 15) and has recently been incorporated into the GHD framework. Since ballistic transport is absent, the dominant transport mechanism is diffusive. The diffusion constant D has been rigorously bounded (46, 47) and computed by using GHD (23–25); D diverges in the isotropic ($\Delta=1$) limit, at which wavepackets spread superdiffusively, with dynamical scaling $x \sim t^{2/3}$ and a non-Gaussian front that matches the Kardar–Parisi–Zhang (KPZ) universality class (18, 48–51). Away from half-filling, the \uparrow and \downarrow domains do not precisely cancel, so magnons do carry magnetization, and

Significance

The XXZ model is a canonical model of quantum magnetism. In one dimension, this model is integrable and has ballistically moving quasiparticles; thus, energy spreads ballistically, but, surprisingly, spin transport can be diffusive or superdiffusive. Here, we show that spin transport is even richer in the presence of a magnetic field: Some fraction of the spin moves out ballistically, but the dynamical spin-structure factor decays with an anomalous, continuously varying exponent. A hitherto-unnoticed phase transition takes place at finite fields, separating ballistic from subballistic decay of local correlations. We analytically derive these results using generalized hydrodynamics and support our findings numerically. These anomalous exponents can readily be measured via the frequency and wavevector dependence of the spin conductivity.

Author contributions: S.G., R.V., and B.W. designed research; S.G., R.V., and B.W. performed research; S.G., R.V., and B.W. analyzed data; and S.G. and R.V. wrote the paper.

The authors declare no conflict of interest.

This article is a PNAS Direct Submission.

Published under the PNAS license.

¹To whom correspondence may be addressed. Email: sarang.gopalakrishnan@csci.cuny.edu.

This article contains supporting information online at www.pnas.org/lookup/suppl/doi:10.1073/pnas.1906914116/-DCSupplemental.

Published online July 30, 2019.

ballistic spin transport is present. Beyond these results, the behavior of the dynamical spin-structure factor in this high-temperature limit are still poorly understood (but see ref. 52). The zero temperature limit has been extensively studied (53–57), and so has the low-energy field theory regime (12, 13, 15, 16, 58), but as we will see, that the physics is qualitatively different at high temperature.

Here, we compute the dynamical spin-structure factor within GHD. We focus on the connected correlation function $C(x, t) \equiv \langle S_{i+x}^z(t) S_i^z(0) \rangle^c$ evaluated at infinite temperature with chemical potential μ ; everything we discuss will involve large x, t but arbitrary x/t . We find that, even away from half-filling, the local behavior of autocorrelators (i.e., for $x/t \ll 1$, corresponding to the return probability) evolves with continuously varying exponents that depend on Δ and h (Fig. 1). There is a phase transition in the (Δ, h) plane, between ballistic (i.e., $C(0, t) \sim 1/t$) and subballistic (i.e., $C(0, t) \sim 1/t^\gamma$ for $1/2 < \gamma < 1$) asymptotic behavior. We compute the exponent γ as a function of (h, Δ) , and show that for $\Delta > 1$ it universally approaches $1/2$ as $h \rightarrow 0$, recovering (and shedding light on) diffusion at half-filling. This coexistence of ballistic and anomalous behavior was recently demonstrated (59) for disordered integrable spin chains (60); here, we show that the same effect occurs in clean, strongly interacting systems. At the Heisenberg point, the phase boundary in the (Δ, h) plane intersects the ballistic–diffusive phase boundary at $h = 0$, and, in this sense, the isotropic Heisenberg point at $h = 0$ is a dynamical multicritical point. We write down a scaling form for the structure factor as one approaches this critical point at finite h .

Low-Filling Limit

Our results have an elementary interpretation in the limit in which the density of \uparrow spins $f \ll 1$. Here, $f \sim e^{2\mu}$ with $\mu \rightarrow -\infty$. Nevertheless, the system is still at infinite temperature. Further, for the present discussion, we take $\Delta \gg 1$. Specifically, we take the double limit $f \rightarrow 0$ and $\Delta \rightarrow \infty$ but assume that the product $f\Delta$ is of order unity; this allows us to calculate the structure factor by elementary methods, invoking integrability only to treat the quasiparticles as stable. In this double limit, the quasiparticles are essentially “bare”: An s -string is a sequence of s \uparrow spins on top of a \downarrow background. The collision rate between quasiparticles depends on the quasiparticle density f , but the scattering phase shift remains finite at large Δ , so the dressing of quasiparticles due to collisions vanishes in the double limit. Meanwhile, although the density of large- s strings decreases exponentially in

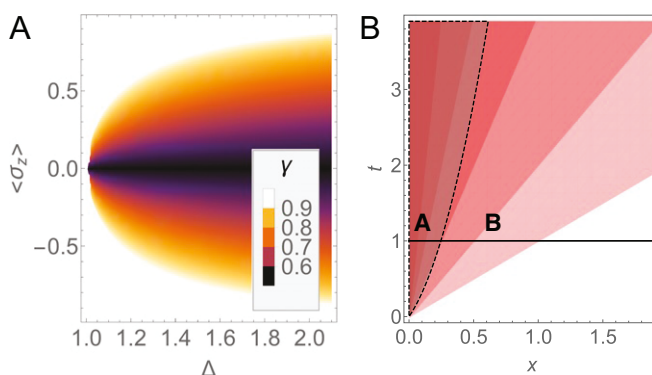


Fig. 1. Return probability. (A) Exponent of the return probability, $C(0, t) \sim t^{-\gamma}$, as a function of the filling and the anisotropy. This result applies for any fixed x as $t \rightarrow \infty$. (B) Mechanism for anomalous local relaxation: The velocity of an s -string in the easy-axis XXZ model decreases exponentially with s . Light strings in region B spread out ballistically; heavy strings in region A move diffusively because of collisions with light strings. As time passes, more strings become “light” in that their motion is chiefly ballistic.

, we will see that all strings contribute to the autocorrelator in the double limit. This is because an s -string can only move at s th order in perturbation theory, so its velocity is $v_s \sim \Delta^{1-s}$. Large- s strings are thus both exponentially rare and exponentially slow, and these two effects compensate each other.

As we argued above, dressing effects are suppressed by uncompensated factors of f and are therefore negligible in the double limit. Therefore, we can treat the contribution of each string to the autocorrelator at the single-particle level. The s -strings have free-particle dispersions of the form

$$\epsilon_s(q) = k_s \Delta^{1-s} \sin(2q), \quad [2]$$

and in this limit the autocorrelation function is that of a gas of s -strings that occur with density f^s and do not interact with one another. A single-particle calculation then yields the structure factor, as follows [see *SI Appendix* for thermodynamic Bethe Ansatz formulas at infinite temperature, details of the low-filling calculation, and more numerical results of matrix product operator (MPO) calculations]:

$$C(x, t) \simeq \sum_{s \geq 1} s^2 f^s [J_x(k_s \Delta^{1-s} t)]^2, \quad [3]$$

where J_x denote Bessel functions of the first kind (61). A non-trivial contribution arises if a string beginning at $(0, 0)$ has propagated to (x, t) . To explore the asymptotics of Eq. 3, we approximate the Bessel function as a step function and ignore irrelevant prefactors, $[J_x(k_s \Delta^{1-s} t)]^2 \sim \Theta(x - \Delta^{1-s} t) \Delta^{s-1}/t$. Fixing a point x , and counting only those s -strings that have reached x by the time t , we get

$$C(x, t) \approx \sum_{s=1}^{s_*} s^2 \frac{f}{t} (f \Delta)^{s-1}, \quad [4]$$

where $s_* = 1 + \log(t/x)/\log \Delta$. There are two cases. When $f\Delta < 1$, contributions from large- s strings are subleading to the $1/t$ tail of the 1-strings. When $f\Delta > 1$, the dominant strings at x are the heaviest strings that have made it there; Eq. 4 is dominated by the term of order s_* , implying

$$C(x, t) \sim \frac{f}{t} \left(\frac{t}{x} \right)^{1 - \frac{|\log f|}{\log \Delta}} \log^2 \left(\frac{t}{x} \right) t \gg x \sim t^{-\frac{2|\mu|}{\eta}} \log^2 t, \quad [5]$$

for $2|\mu| < \eta$. The exponent $\gamma = \frac{2|\mu|}{\eta}$ in Eq. 5 goes to unity as $\eta \gg |\mu|$, suggesting subdiffusion ($\gamma < \frac{1}{2}$) as $\Delta \rightarrow \infty$ at the Eulerian level.

The asymptotics 5 arises because, in the double limit, long strings are effectively stationary for exponentially long times. We now turn to the leading corrections to this limit, by allowing terms with one uncompensated factor of f . Thus, we allow for the scattering between all s -strings and the relatively abundant 1-strings, which have density $\sim f$. This process will be sufficient to prevent subdiffusion. In general, when a q -string and an $s > q$ -string collide, the s -string picks up a displacement of $2q$ sites (62, 63). Thus, all strings undergo subleading diffusive motion from random collisions. In the low-density limit, the diffusion constant is set by the density of 1-strings and thus scales as $D \sim f$. Because the model is integrable, diffusion takes place in addition to the ballistic motion of s -strings. At intermediate times, an s -string moves diffusively; it crosses over to ballistic motion at times such that $\sqrt{ft} < \Delta^{1-s} t$, i.e., for strings satisfying

$$s \gtrsim s_0(t) \sim 1 + \frac{|\log(ft)|}{2 \log \Delta}. \quad [6]$$

When $f\Delta < 1$, heavy strings are sparse, so it does not matter whether they diffuse. When $f\Delta > 1$, Euler-scale results remain valid at distances $x \gtrsim x_0 \equiv \sqrt{f}t$, but the behavior for $x \lesssim x_0$ is qualitatively modified, as heavy strings are diffusive, not immobile. Thus, the autocorrelator decays as

$$C(x \lesssim x_0, t) \sim t^{-\frac{1}{2} - \frac{|\mu|}{\eta}} \log^2 t, \quad 2|\mu| < \eta. \quad [7]$$

The slowest that $C(x, t)$ can decay is as $1/\sqrt{t}$; i.e., a subdiffusive decay of the return probability does not occur in this model. Instead, the generic behavior is an anomalous decay with a continuously varying power law between $\frac{1}{2}$ and 1.

Generic Filling

The above elementary argument is restricted to large Δ and low filling. We now show that our main conclusion—the anomalous decay 7 of the local autocorrelation function—holds generally for all h whenever $\Delta > 1$. Generally, spin transport can still be understood in terms of a hierarchy of strings, but their interactions are now important, and their velocity and effective charge are dressed by the collisions with one another. These issues can be addressed by using GHD: Since we are dealing with a linear response problem, we take advantage of the fact that the quasiparticles are in local thermal equilibrium and evaluate the dressed quasiparticle dispersion and quasiparticle distribution function using data from the thermodynamic Bethe ansatz solution. Then, the hydrodynamic expression for the structure factor takes the form (29, 33):

$$C(x, t) = \sum_{s=1}^{\infty} \int du \rho_s^{\text{tot}}(u) \theta_s(1 - \theta_s) (m_s^{\text{dr}})^2 \varphi_t[x - v_s(u)t], \quad [8]$$

where u parameterizes the rapidity of a quasiparticle; m_s^{dr} is the dressed magnetization of string s ; $\rho_s^{\text{tot}}(u)$ is the available density of states; θ_s is its occupation number (Fermi factor); and v_s is its effective velocity. These quantities have closed-form expressions for generic μ at infinite temperature (11, 47) (see *SI Appendix* for thermodynamic Bethe Ansatz formulas at infinite temperature, details of the low-filling calculation, and more numerical results of MPO calculations). Finally, the function $\varphi_t(\zeta)$ is the propagator of a string with quantum numbers (s, u) from $(0, 0)$ to (x, t) . At the Euler level, this propagator would simply be a Dirac delta

function. In principle, the full form of $C(x, t)$, including diffusive corrections and possible nonlinearities, could be ascertained from flea-gas simulations (32). Here, we are interested in the asymptotic behavior of this quantity. We therefore include the dominant “diagonal” diffusive corrections by broadening $\varphi_t(\zeta)$ to a Gaussian with variance $2D_s(\eta, u)t$. The diagonal quasiparticle diffusion constant $D_s(\eta, u)$ was computed in refs. 21 and 22 and can be evaluated numerically. We can check explicitly that our hydrodynamic form for the structure factor 8 is consistent with the exact sum rule

$$\int_{-\infty}^{\infty} dx C(x, t) = \frac{1}{4}(1 - \tanh^2 \mu), \quad [9]$$

since the function $\varphi_t(\zeta)$ is normalized to unity (see *SI Appendix* for thermodynamic Bethe Ansatz formulas at infinite temperature, details of the low-filling calculation, and more numerical results of MPO calculations).

This GHD expression gives a closed-form result for local relaxation—i.e., $C(x, t)$ at fixed large x when $t \rightarrow \infty$. There are two contributions at time t , from light strings (whose motion is primarily ballistic) and from heavy strings (which undergo Brownian motion from collisions with light strings). Regardless of μ , the velocities of very heavy strings scale as $v_s \simeq e^{-\eta s}$; also, at infinite temperature, their densities scale as $\rho_s(u) = \rho_s^{\text{tot}}(u)\theta_s \sim e^{-2|\mu|s}$ (23). The dressed magnetization of the heavy strings, meanwhile, is the same as the bare magnetization $m_s^{\text{dr}} \simeq s$. We see that the asymptotics of v_s and ρ_s are identical to the low-filling limit: For $\eta > 2|\mu|$, the return probability is dominated by the diffusive strings, $s > s_0(t)$, where $s_0(t) \simeq \frac{1}{2\eta} \log t$. It follows that Eq. 7 applies for all μ and $\eta > 1$. (Note, however, that away from the perturbative limit, $\eta \neq \log \Delta$.)

For a fixed $\eta > 0$ and $\mu < \eta/2$, this asymptotic scaling sets in on timescales $t \gtrsim e^{2\eta/|\mu|}$; at shorter times, we expect a smaller apparent exponent, since the dominant strings at those times are not yet exponentially suppressed (Fig. 2).

Properties Near Half-Filling

Near half-filling—i.e., for $\mu \ll 1$ —we can extract more quantitative information about the structure factor. Again, we classify strings as light and heavy at time t , depending on whether their spread up to time t is primarily ballistic or diffusive. For light strings, diffusive corrections are a subleading effect (except at the front), so we treat light strings at the Euler level. For heavy

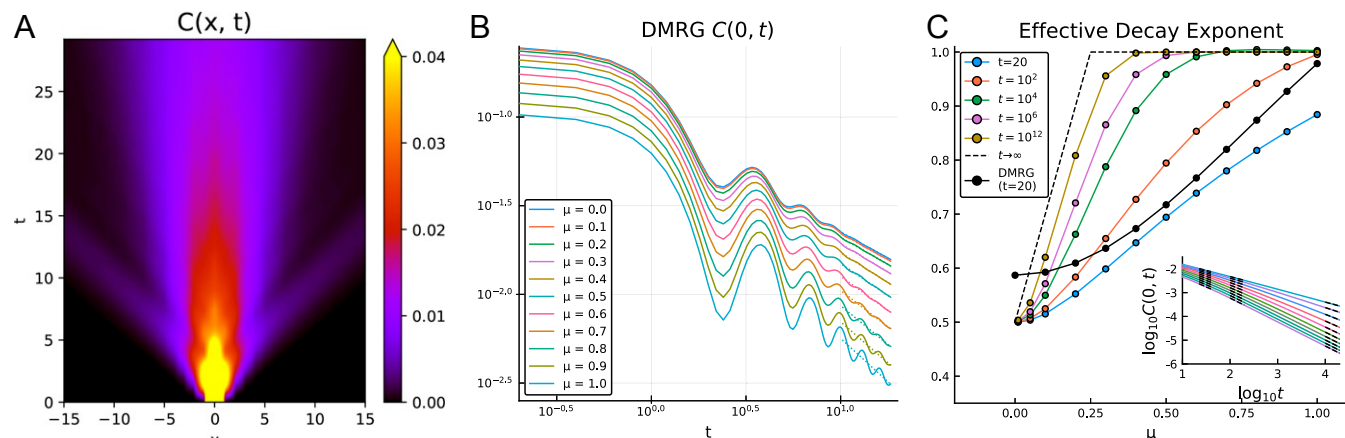


Fig. 2. Simulations of the structure factor. (A) Spacetime plot of the spectral intensity computed via the MPO method, for $\eta = 1.5$, $\mu = 0.5$, indicating a ballistically moving peak due to magnons and a slow background to heavier strings. (B) MPO simulations of the return probability vs. μ at fixed $\eta = 0.5$; the exponent is initially close to diffusive, then shifts downward with increasing μ . (C) Comparison of exponents extracted from the MPO simulations to those computed by numerical evaluation of Eq. 8 using various fitting windows. Evidently, the GHD result is quite slow to converge to its late-time asymptotic behavior.

strings near half-filling, the diffusive broadening constant has the closed-form expression

$$D = \frac{2 \sinh \eta}{9\pi} \sum_{s=1}^{\infty} (1+s) \left[\frac{s+2}{\sinh \eta s} - \frac{s}{\sinh \eta (s+2)} \right], \quad [10]$$

which coincides with the spin-diffusion constant (23–25). This expression is a sum over contributions from s -strings, and only strings with $s\eta \lesssim 1$ contribute. This expression also applies for $\mu < \eta \ll 1$, since a nonzero μ only affects strings with $s > 1/\mu > 1/\eta$, whose contributions to Eq. 10 are anyway exponentially suppressed.

We now discuss the behavior of $C(x, t)$ near half-filling along rays with $x/t \neq 0$. For nonzero μ , at late times, there are two different types of ballistic strings, depending on the size of $s\mu$. When $s\mu \gg 1$, the ballistic strings behave as in the low-filling limit: Their density and velocity are both exponentially suppressed, and we recover Eq. 5. However, for lighter strings with $s\mu \lesssim 1$, the density is only suppressed algebraically as $\rho_s \simeq 1/s^3$, while the velocity is suppressed exponentially $v_s \simeq e^{-\eta s}$. Therefore, at a fixed x , the largest string that has made it out to x has index $s_* = \log(t/x)/\eta$. The density of such strings is $1/s_*^3$, while each carries a small dressed magnetization $s_*^2 \mu$. Thus, in this regime, we have

$$C(x, t) \sim \frac{\mu^2}{\eta} \frac{\log(t/x)}{x}, \quad e^{-\eta/|\mu|} \ll \frac{x}{t} \ll 1, \quad [11]$$

where the regime of validity of this result is controlled by μ and is to be understood on a logarithmic scale for x/t . At a fixed x , therefore, $C(x, t)$ first grows logarithmically with time, as heavier strings carrying more magnetization appear at x . Then, at a timescale $t \sim x e^{-\eta/|\mu|}$, the correlator begins to decay with the Eulerian exponent 5, and finally crosses over to the asymptotic behavior 7 when $t \sim x^2/D$.

Exactly at half-filling ($\mu = 0$), the structure factor simplifies even further. All strings but the heaviest ones $s \rightarrow \infty$ become effectively neutral as $m_s^{\text{dr}} \sim s^2 \mu$ goes to 0 for $s \ll \mu^{-1}$, so the structure factor reads

$$C(x, t) = \frac{1}{4} \varphi_t(x) = \frac{1}{8\sqrt{\pi D(\eta)} t} e^{-\frac{x^2}{4D(\eta)t}}, \quad [12]$$

where we have used the sum rule 9 at half-filling, and $v_\infty = 0$. At half-filling, the structure factor is thus given by the heaviest strings (23), which are moving purely diffusively because of random collisions with lighter strings, with the spin diffusion constant 10.

Isotropic Point

Finally, we briefly discuss the structure factor at the isotropic point $\eta = 0$ ($\Delta = 1$). At half-filling, Eq. 10 implies that the diffusion constant diverges with the number of strings as $D \sim s$. Spin transport at half-filling is therefore superdiffusive, with anomalous dynamical exponent $x \sim t^{2/3}$. By considering the approach to half-filling at finite μ , one can retrieve this dynamical exponent by a simple intuitive argument. A typical thermal state has Gaussian spatial fluctuations of its magnetization, so the effective local magnetization fluctuates as $1/\sqrt{L}$ over a distance L . On short enough length-scales, these fluctuations dominate over the average μ . The system averages out these fluctuations and “realizes” it is at $\mu \neq 0$ on a length-scale such that $\mu \sim 1/\sqrt{L}$ —i.e., $L(\mu) \sim 1/\mu^2$. Further, as $\mu \rightarrow 0$, magnetization is primarily transported by the heaviest available strings, for which $s_* \simeq 1/\mu$ and $v_{s_*} \simeq \mu$. The time it takes these strings to travel a distance

$L(\mu)$ is given by $t(\mu) \sim 1/\mu^3$. The diffusion constant of such strings diverges as $D \sim \mu^{-1}$, which also gives the same scaling $t(\mu) \sim 1/\mu^3$. It follows that $L \sim t^{2/3}$. Moreover, the structure factor near half-filling can be written in the scaling form

$$C(x, t) = \mu^2 \left[C_{\text{anom.}}(x\mu^2, t\mu^3) + \frac{1}{t} C_{\text{reg.}}(x/t) \right], \quad [13]$$

where the first term comes from strings with $s^* \sim 1/\mu$ and the second from lighter strings. At precisely half-filling, the regular part vanishes as μ^2 , and only the anomalous part survives. The regimes of $C_{\text{anom.}}(\zeta, \xi)$ are as follows. When both $\zeta, \xi \ll 1$, $C_{\text{anom.}} \sim (t\mu^3)^{-2/3} f(x/t^{2/3})$, where f was numerically found to have the KPZ form (49). When $\zeta \gg \xi$, the anomalous part vanishes by causality. The late-time return probability $\xi \gg 1$, $\zeta \ll \xi$ is dominated by the tail of the heaviest common string—i.e., it goes as $1/(\mu t)$. Putting these together, we have

$$C(0, t) = t^{-2/3} g(\mu t^{1/3}), \quad g(y) = \begin{cases} \text{const.} & y \ll 1 \\ 1/y & y \gg 1 \end{cases} \quad [14]$$

Meanwhile, the ballistic, regular part can be calculated following the logic of Eq. 11, so $C_{\text{reg.}}(y) \sim 1/y^2$ for $y \ll 1$, implying that

$$C(x/t) \sim \mu^2 t/x^2, \quad \mu \ll (x/t) \ll 1. \quad [15]$$

As $\mu \rightarrow 0$, spatial fluctuations of the magnetization dominate the dynamics. If we imagine dividing the system into hydrodynamic cells with magnetization $m(x, t)$, each cell will have a fluctuating diffusion constant $D[m] \sim 1/m$ and ballistic spin transport coefficient $j_{\text{ballistic}}[m] \sim v[m]m \sim m^2$ set by its instantaneous magnetization (repeating the argument above with m instead of μ as the cutoff). Combining these contributions into a hydrodynamic equation for m yields a Burgers equation with a diffusion constant that is singular at low density (see also ref. 25). We expect this to be compatible with KPZ scaling (50): Over a distance ℓ , Gaussian fluctuations in the initial state lead to $m \sim 1/\sqrt{\ell}$, implying a diffusion constant $D \sim \sqrt{\ell}$ and velocity $v \sim 1/\sqrt{\ell}$, both implying $t(\ell) \sim \ell^{3/2}$. Moreover, the dominant nonlinearities in the Burgers equation involve anomalous high-density regions, for which the diffusion coefficient is well-behaved, so one might conjecture that the KPZ scaling function is also unaffected, as the numerical evidence (49) suggests. However, developing this nonlinear fluctuating hydrodynamics (64) for integrable systems is outside the scope of the present work.

Matrix Product Operator Calculations

We tested these predictions by computing the structure factor $C(x, t)$ in the Heisenberg picture by time evolving S_i^z using MPO techniques and the time-dependent density matrix renormalization group (tDMRG) (65–69) (Materials and Methods). Following ref. 49 (see also refs. 70 and 71), we also computed $C(x, t)$ using a linear response quench setup when the system was initially prepared in a nonequilibrium state with chemical potential $\mu + \delta\mu/2$ in the left half of the system and $\mu - \delta\mu/2$ in the right half. We then computed the density matrix $\rho(t)$ at time t using MPO methods. Working at fixed truncation error, this approach allows us to reach similar time scales $t \sim 20$ to obtain fully converged results. If we work instead with fixed bond dimension MPOs, the quench time traces deviate from the exact MPO time trace at times $t \lesssim 20$ for the return probability, though they give reasonably converged spatial profiles for $x \neq 0$ out to late times (see *SI Appendix* for thermodynamic Bethe Ansatz formulas at infinite temperature, details of the low-filling calculation, and more numerical results of MPO calculations), as noted in refs. 18 and 49.

These results are plotted in Fig. 2. For $\mu = 0.5$ and $\eta = 1.5$, one sees a clear ballistic front due to magnons, with a broad diffuse feature behind it, as GHD predicts. Fig. 2B shows the local autocorrelator (i.e., return probability) as a function of μ at fixed $\eta = 0.5$. Its behavior is consistent with a continuously varying power law that goes from $\sim 1/2$ (in fact, closer to 0.6 due to the proximity to the isotropic point $\Delta = 1$) at $\mu = 0$ to nearly one at large μ . The numerically extracted exponent γ is much smaller than the asymptotic GHD prediction. We accounted for this discrepancy by numerically evaluating the GHD expression, Eq. 8. As discussed above, GHD predicts that the apparent exponent drifts with time (Fig. 2C). If we fit the GHD prediction to a power law over timescales $t \approx 20$, we find that the GHD and MPO exponents are in reasonable agreement. Note that GHD is not expected to be quantitatively accurate at such short times, as it does not capture the oscillations observed numerically. Although much longer times would be needed to test the asymptotics Eq. 7, our numerical results are consistent with a continuously evolving exponent between $\frac{1}{2}$ and 1.

Discussion

In this work, we used GHD and its diffusive corrections to characterize the structure factor of the XXZ model in the easy-axis regime and at the isotropic Heisenberg point. We argued that even at nonzero magnetization, where ballistic transport is present, the local behavior of the autocorrelation function exhibits rich structure due to heavy “string” quasiparticles. In particular, the autocorrelation function for $x \ll \sqrt{Dt}$ —i.e., the “return probability”—vanishes with an anomalous exponent $\gamma = \min(\frac{1}{2} + \frac{|\mu|}{\eta}, 1)$ throughout this phase. In many experimental situations, it is more natural to consider Fourier-transformed variables—i.e., to evaluate the dynamical structure factor $S(q, \omega)$ (which is the Fourier transform of $C(x, t)$)—and behaves as (see *SI Appendix* for thermodynamic Bethe Ansatz formulas at infinite temperature, details of the low-filling calculation, and more numerical results of MPO calculations)

$$S(q, \omega) = \frac{Dq^2(Dq)^{2|\mu|/\eta} \log^2(Dq)}{\omega^2 + (Dq^2)^2} + S_b, \quad [16]$$

where the contribution S_b comes from ballistic strings and is subleading when $\omega \ll Dq^2$ and $2|\mu| < \eta$. The optical conductivity follows from this as $\sigma(q, \omega) = (\omega/q)^2 S(q, \omega)$. At a fixed q , the ω -dependence is regular, being a sum of ballistic and diffusive contributions; however, fixed- x correlators behave nonanalytically because of the integral over q .

Our predictions based on GHD are consistent with extensive simulations using MPO methods (Fig. 2). In addition, at the isotropic point, we wrote down a scaling form for the structure factor and provided an elementary derivation of the dynamical critical exponent (24, 25). While our results have a particularly simple form at $T = \infty$, the main qualitative features persist for all $T > 0$. Many possible extensions present themselves, including a systematic derivation of fluctuating hydrodynamics and

long-time tails near half-filling and an understanding of the scaling properties as one approaches $\Delta \rightarrow 1$ from the easy-plane (“gapless”) regime.

Materials and Methods

We have explored two approaches for computing the structure factor $C(x, t) = \langle S_x^z(t) S_0^z(0) \rangle^c$ numerically. The first is to directly time-evolve the operator S_z in the Heisenberg picture, as an MPO and the tDMRG (65–69). We find that a fixed truncation error $\epsilon = 10^{-8}$ is enough to obtain converged results, and we used a fourth-order Trotter decomposition with time step $dt = 0.1$. Our calculations were stopped when the bond dimension reached $\chi \sim 2,000$. This approach corresponds precisely to performing the linear response calculation, so we refer to it as the equilibrium approach. In addition to being strictly in the linear response regime, the equilibrium approach has the advantage that one can study μ -dependence systematically with minimal computational effort: Since $C(x, t, \mu) = \text{Tr}[e^{-2 \sum_i \mu S_i^z(t) S_0^z(0)} / Z - \langle S_z^2 \rangle]$, the MPO $S_x^z(t)$ only needs to be computed once. In practice, this computation can be further sped up (72) by instead evaluating $\text{Tr}[e^{-2 \sum_i \mu S_i^z(t/2) S_0^z(-t/2)}]$. These MPOs are only evolved for half as long and therefore have much lower bond dimension than $S_x^z(t)$.

Instead of this direct method, the structure factor can also be computed by using a linear-response quantum quench. Following ref. 49, we considered an initial density matrix $\rho(t=0) \propto (e^{(\mu + \delta\mu/2)\sigma_z} \otimes I^L)^{1/2} \otimes (e^{(\mu - \delta\mu/2)\sigma_z})^{\otimes L/2}$. The equilibrium (connected) spin-structure factor can then be expressed as (49)

$$C(x, t) = \frac{1}{4} \lim_{\delta\mu \rightarrow 0} \frac{\langle \sigma_{x-1}^z(t) \rangle_{\text{quench}} - \langle \sigma_x^z(t) \rangle_{\text{quench}}}{\delta\mu}, \quad [17]$$

where $\langle \dots \rangle_{\text{quench}}$ refers to expectation values in this quench setting. We used MPO methods to time-evolve the initial density matrix $\rho(t=0)$ and to evaluate expectation values of the spin. This provides another way to compute the spin-structure factor. The quench setup could possibly allow us to reach longer times. While the bond dimension appears to grow more slowly in the quench setting, we find that very small truncation errors (less than $\epsilon = 10^{-10}$) are required to obtain converged results for the return probability ($x = 0$) for $\delta\mu = 0.01$ (a value small enough to make Eq. 17 correct up to negligible errors). On the other hand, as noted in refs. 18 and 49, working with fixed bond dimension χ in the quench setup (with bond dimensions $\chi = 100, 200, 300, 400$) appears to lead to relatively small errors for small values of η , yielding reasonably converged results for the full shape of $C(x, t)$ up to very long times $t \sim 200$ —especially near the front, where truncation errors are less important. In contrast, the return probability $C(x=0, t)$ does seem sensitive to truncation errors, and even fixed $\chi = 400$ appears to deviate from the numerically exact equilibrium result at short times $t \sim 15$ (*SI Appendix*). In this work, we thus used the quench setup with fixed bond dimension to compute the full profile of $C(x, t)$, as this yields reasonably converged results away from $x = 0$ up to long times, and we restricted ourselves to fixed truncation error data computed directly in equilibrium for the return probability.

ACKNOWLEDGMENTS. We thank Vincenzo Alba, Jacopo De Nardis, David Huse, Christoph Karrasch, and Vadim Oganesyan for helpful discussions. This work was supported by NSF Grant DMR-1653271 (to S.G.); and US Department of Energy Office of Science, Basic Energy Sciences, Early Career Award DE-SC0019168 (to R.V.). We thank the Kavli Institute for Theoretical Physics, which is supported by the National Science Foundation under Grant NSF PHY-1748958, and the Program “The Dynamics of Quantum Information,” where part of this work was performed.

1. T. Kinoshita, T. Wenger, D. Weiss, A quantum Newton’s cradle. *Nature* **440**, 900–903 (2006).
2. S. Hild *et al.*, Far-from-equilibrium spin transport in Heisenberg quantum magnets. *Phys. Rev. Lett.* **113**, 147205 (2014).
3. M. Rigol, V. Dunjko, M. Olshanii, Thermalization and its mechanism for generic isolated quantum systems. *Nature* **452**, 854–858 (2008).
4. J. S. Caux, F. H. L. Essler, Time evolution of local observables after quenching to an integrable model. *Phys. Rev. Lett.* **110**, 257203 (2013).
5. E. Ilievski, M. Medenjak, T. Prosen, L. Zadnik, Quasilocal charges in integrable lattice systems. *J. Stat. Mech. Theory Exp.* **2016**, 064008 (2016).
6. E. Ilievski *et al.*, Complete generalized Gibbs ensembles in an interacting theory. *Phys. Rev. Lett.* **115**, 157201 (2015).
7. B. Pozsgay *et al.*, Correlations after quantum quenches in the xxz spin chain: Failure of the generalized Gibbs ensemble. *Phys. Rev. Lett.* **113**, 117203 (2014).
8. M. Gring *et al.*, Relaxation and prethermalization in an isolated quantum system. *Science* **337**, 1318–1322 (2012).
9. T. Langen, T. Gasenzer, J. Schmiedmayer, Prethermalization and universal dynamics in near-integrable quantum systems. *arXiv:1603.09385* e-prints (30 March 2016).
10. Y. Tang *et al.*, Thermalization near integrability in a dipolar quantum Newton’s cradle. *Phys. Rev. X* **8**, 021030 (2018).
11. M. Takahashi, *Thermodynamics of One-Dimensional Solvable Models* (Cambridge Univ Press, Cambridge, UK, 1999).
12. S. Sachdev, K. Damle, Low temperature spin diffusion in the one-dimensional quantum o(3) nonlinear σ model. *Phys. Rev. Lett.* **78**, 943–946 (1997).
13. K. Damle, S. Sachdev, Spin dynamics and transport in gapped one-dimensional Heisenberg antiferromagnets at nonzero temperatures. *Phys. Rev. B* **57**, 8307–8339 (1998).

14. X. Zotos, Finite temperature Drude weight of the one-dimensional spin-1/2 Heisenberg model. *Phys. Rev. Lett.* **82**, 1764–1767 (1999).
15. K. Damle, S. Sachdev, Universal relaxational dynamics of gapped one-dimensional models in the quantum Sine-Gordon universality class. *Phys. Rev. Lett.* **95**, 187201 (2005).
16. J. Sirker, R. G. Pereira, I. Affleck, Diffusion and ballistic transport in one-dimensional quantum systems. *Phys. Rev. Lett.* **103**, 216602 (2009).
17. C. Karrasch, J. E. Moore, F. Heidrich-Meisner, Real-time and real-space spin and energy dynamics in one-dimensional spin- $\frac{1}{2}$ systems induced by local quantum quenches at finite temperatures. *Phys. Rev. B* **89**, 075139 (2014).
18. M. Ljubotina, M. Žnidarič, T. Prosen, Spin diffusion from an inhomogeneous quench in an integrable system. *Nat. Commun.* **8**, 16117 (2017).
19. L. Piroli, J. De Nardis, M. Collura, B. Bertini, M. Fagotti, Transport in out-of-equilibrium XXZ chains: Nonballistic behavior and correlation functions. *Phys. Rev. B* **96**, 115124 (2017).
20. B. Bertini, L. Piroli, Low-temperature transport in out-of-equilibrium XXZ chains. *J. Stat. Mech. Theory Exp.* **2018**, 033104 (2018).
21. J. De Nardis, D. Bernard, B. Doyon, Hydrodynamic diffusion in integrable systems. *Phys. Rev. Lett.* **121**, 160603 (2018).
22. S. Gopalakrishnan, D. A. Huse, V. Khemani, R. Vasseur, Hydrodynamics of operator spreading and quasiparticle diffusion in interacting integrable systems. *Phys. Rev. B* **98**, 220303 (2018).
23. J. De Nardis, D. Bernard, B. Doyon, Diffusion in generalized hydrodynamics and quasiparticle scattering. arXiv:1812.00767 (3 December 2018).
24. S. Gopalakrishnan, R. Vasseur, Kinetic theory of spin diffusion and superdiffusion in xxz spin chains. *Phys. Rev. Lett.* **122**, 127202 (2019).
25. J. De Nardis, M. Medenjak, C. Karrasch, E. Ilievski, Anomalous spin diffusion in one-dimensional antiferromagnets. arXiv:1903.07598 (18 March 2019).
26. O. A. Castro-Alvaredo, B. Doyon, T. Yoshimura, Emergent hydrodynamics in integrable quantum systems out of equilibrium. *Phys. Rev. X* **6**, 041065 (2016).
27. B. Bertini, M. Collura, J. De Nardis, M. Fagotti, Transport in out-of-equilibrium xxz chains: Exact profiles of charges and currents. *Phys. Rev. Lett.* **117**, 207201 (2016).
28. B. Doyon, T. Yoshimura, A note on generalized hydrodynamics: Inhomogeneous fields and other concepts. *SciPost Phys.* **2**, 014 (2017).
29. B. Doyon, H. Spohn, Drude weight for the Lieb-Liniger Bose gas. *SciPost Phys.* **3**, 039 (2017).
30. E. Ilievski, J. De Nardis, Microscopic origin of ideal conductivity in integrable quantum models. *Phys. Rev. Lett.* **119**, 020602 (2017).
31. V. B. Bulchandani, R. Vasseur, C. Karrasch, J. E. Moore, Bethe-Boltzmann hydrodynamics and spin transport in the XXZ chain. *Phys. Rev. B* **97**, 045407 (2018).
32. B. Doyon, T. Yoshimura, J. S. Caux, Soliton gases and generalized hydrodynamics. *Phys. Rev. Lett.* **120**, 045301 (2018).
33. E. Ilievski, J. De Nardis, Ballistic transport in the one-dimensional Hubbard model: The hydrodynamic approach. *Phys. Rev. B* **96**, 081118 (2017).
34. M. Collura, A. De Luca, J. Viti, Analytic solution of the domain-wall nonequilibrium stationary state. *Phys. Rev. B* **97**, 081111 (2018).
35. V. Alba, P. Calabrese, Entanglement and thermodynamics after a quantum quench in integrable systems. *Proc. Natl. Acad. Sci. U.S.A.* **114**, 7947–7951 (2017).
36. A. De Luca, M. Collura, J. De Nardis, Nonequilibrium spin transport in integrable spin chains: Persistent currents and emergence of magnetic domains. *Phys. Rev. B* **96**, 020403 (2017).
37. V. B. Bulchandani, R. Vasseur, C. Karrasch, J. E. Moore, Solvable hydrodynamics of quantum integrable systems. *Phys. Rev. Lett.* **119**, 220604 (2017).
38. V. B. Bulchandani, On classical integrability of the hydrodynamics of quantum integrable systems. *J. Phys. A Math. Theor.* **50**, 435203 (2017).
39. B. Doyon, J. Dubail, R. Konik, T. Yoshimura, Large-scale description of interacting one-dimensional Bose gases: Generalized hydrodynamics supersedes conventional hydrodynamics. *Phys. Rev. Lett.* **119**, 195301 (2017).
40. J. S. Caux, B. Doyon, J. Dubail, R. Konik, T. Yoshimura, Hydrodynamics of the interacting Bose gas in the quantum Newton cradle setup. arXiv:1711.00873 (2 November 2017).
41. X. Cao, V. B. Bulchandani, J. E. Moore, Incomplete thermalization from trap-induced integrability breaking: Lessons from classical hard rods. *Phys. Rev. Lett.* **120**, 164101 (2018).
42. B. Doyon, Exact large-scale correlations in integrable systems out of equilibrium. *SciPost Phys.* **5**, 054 (2018).
43. M. Schemmer, I. Bouchoule, B. Doyon, J. Dubail, Generalized hydrodynamics on an atom chip. *Phys. Rev. Lett.* **122**, 090601 (2019).
44. V. Alba, B. Bertini, M. Fagotti, Entanglement evolution and generalised hydrodynamics: Interacting integrable systems. arXiv:1903.00467 (1 March 2019).
45. L. Bonnes, F. H. L. Essler, A. M. Läuchli, “Light-cone” dynamics after quantum quenches in spin chains. *Phys. Rev. Lett.* **113**, 187203 (2014).
46. M. Medenjak, C. Karrasch, T. Prosen, Lower bounding diffusion constant by the curvature of Drude weight. *Phys. Rev. Lett.* **119**, 080602 (2017).
47. E. Ilievski, J. De Nardis, M. Medenjak, T. Prosen, Superdiffusion in one-dimensional quantum lattice models. *Phys. Rev. Lett.* **121**, 230602 (2018).
48. M. Žnidarič, Spin transport in a one-dimensional anisotropic Heisenberg model. *Phys. Rev. Lett.* **106**, 220601 (2011).
49. M. Ljubotina, M. Žnidarič, T. Prosen, Kardar-Parisi-Zhang physics in the quantum Heisenberg magnet. arXiv:1903.01329 (4 March 2019).
50. M. Kardar, G. Parisi, Y. C. Zhang, Dynamic scaling of growing interfaces. *Phys. Rev. Lett.* **56**, 889–892 (1986).
51. J. Quastel, H. Spohn, The one-dimensional KPZ equation and its universality class. *J. Stat. Phys.* **160**, 965–984 (2015).
52. R. J. Sánchez, V. K. Varma, V. Oganesyan, Anomalous and regular transport in spin-1/2 chains: AC conductivity. *Phys. Rev. B* **98**, 054415 (2018).
53. J. S. Caux, J. M. Maillet, Computation of dynamical correlation functions of Heisenberg chains in a magnetic field. *Phys. Rev. Lett.* **95**, 077201 (2005).
54. R. G. Pereira *et al.*, Dynamical spin structure factor for the anisotropic spin-1/2 Heisenberg chain. *Phys. Rev. Lett.* **96**, 257202 (2006).
55. R. Pereira *et al.*, Dynamical structure factor at small q for the XXZ spin-1/2 chain. *J. Stat. Mech. Theory Exp.* **2007**, P08022 (2007).
56. J. Sirker *et al.*, Boson decay and the dynamical structure factor for the XXZ chain at finite magnetic field. *Phys. B Condens. Matter* **403**, 1520–1522 (2008).
57. A. Klauser, J. Mossel, J. S. Caux, J. van den Brink, Spin-exchange dynamical structure factor of the $s = 1/2$ Heisenberg chain. *Phys. Rev. Lett.* **106**, 157205 (2011).
58. J. Sirker, R. G. Pereira, I. Affleck, Conservation laws, integrability, and transport in one-dimensional quantum systems. *Phys. Rev. B* **83**, 035115 (2011).
59. U. Agrawal, S. Gopalakrishnan, R. Vasseur, Generalized hydrodynamics, quasiparticle diffusion, and anomalous local relaxation in random integrable spin chains. arXiv:1903.03122 (7 March 2019).
60. F. H. L. Essler, R. van den Berg, V. Gritsev, Integrable spin chains with random interactions. *Phys. Rev. B* **98**, 024203 (2018).
61. T. Fukuhara *et al.*, Quantum dynamics of a mobile spin impurity. *Nat. Phys.* **9**, 235–241 (2013).
62. M. Ganahl, M. Haque, H. Evertz, Quantum bowling: Particle-hole transmutation in one-dimensional strongly interacting lattice models. arXiv:1302.2667 (11 February 2013).
63. R. Vlijm *et al.*, Quasi-soliton scattering in quantum spin chains. *Phys. Rev. B* **92**, 214427 (2015).
64. C. B. Mendl, H. Spohn, Dynamic correlators of Fermi-Pasta-Ulam chains and nonlinear fluctuating hydrodynamics. *Phys. Rev. Lett.* **111**, 230601 (2013).
65. S. R. White, A. Feiguin, Real-time evolution using the density matrix renormalization group. *Phys. Rev. Lett.* **93**, 076401 (2004).
66. G. Vidal, Efficient classical simulation of slightly entangled quantum computations. *Phys. Rev. Lett.* **91**, 147902 (2003).
67. U. Schollwoeck, The density-matrix renormalization group in the age of matrix product states. *Ann. Phys.* **326**, 96–192 (2011).
68. C. Karrasch, J. H. Bardarson, J. E. Moore, Finite-temperature dynamical density matrix renormalization group and the Drude weight of spin-1/2 chains. *Phys. Rev. Lett.* **108**, 227206 (2012).
69. C. Karrasch, J. H. Bardarson, J. E. Moore, Reducing the numerical effort of finite-temperature density matrix renormalization group calculations. *New J. Phys.* **15**, 083031 (2013).
70. R. Vasseur, C. Karrasch, J. E. Moore, Expansion potentials for exact far-from-equilibrium spreading of particles and energy. *Phys. Rev. Lett.* **115**, 267201 (2015).
71. C. Karrasch, Hubbard-to-Heisenberg crossover (and efficient computation) of Drude weights at low temperatures. *New J. Phys.* **19**, 033027 (2017).
72. D. Kennes, C. Karrasch, Extending the range of real time density matrix renormalization group simulations. *Comput. Phys. Commun.* **200**, 37–43 (2016).